Rtp1p Is a Karyopherin-Like Protein Required for RNA Polymerase II Biogenesis

Natalia Gómez-Navarro,[a] Lorena Peiró-Chova,[a]* Susana Rodriguez-Navarro,[b] Julio Polaina,[c] Francisco Estruch[a]

Departamento de Bioquímica y Biología Molecular, Facultad de Biología, Universitat de València, Burjassot, Spain[a]; Centro de Investigación Príncipe Felipe, Valencia, Spain[b]; Departamento de Biotecnología, IATA (CSIC), Paterna, Spain[c]

The assembly and nuclear transport of RNA polymerase II (RNA pol II) are processes that require the participation of many auxiliary factors. In a yeast genetic screen, we identified a previously uncharacterized gene, *YMR185w* (renamed *RTP1*), which encodes a protein required for the nuclear import of RNA pol II. Using protein affinity purification coupled to mass spectrometry, we identified interactions between Rtp1p and members of the R2TP complex. Rtp1p also interacts, to a different extent, with several RNA pol II subunits. The pattern of interactions is compatible with a role for Rtp1p as an assembly factor that participates in the formation of the Rpb2/Rpb3 subassembly complex and its binding to the Rpb1p-containing subcomplex. Besides, Rtp1p has a molecular architecture characteristic of karyopherins, composed of HEAT repeats, and is able to interact with phenylalanine-glycine-containing nucleoporins. Our results define Rtp1p as a new component of the RNA pol II biogenesis machinery that plays roles in subunit assembly and likely in transport through the nuclear pore complex.

In eukaryotes, RNA polymerase II (RNA pol II) synthesizes mRNA and several noncoding RNAs. RNA pol II is a multisubunit enzyme composed of 12 subunits that are highly conserved among eukaryotes and whose structure has been well characterized (1). Yeast RNA pol II can dissociate into a 10-subunit catalytic core and a heterodimer of subunits Rpb4p and Rpb7p, which are required for the initiation from promoter DNA (2). The two large subunits, Rpb1p and Rpb2p, form the central mass of the enzyme, whereas the smaller subunits generally bind on the surface. Although the structure and functional regulation of RNA pol II have been characterized in detail, the study of its biogenesis has only recently been pursued. By assuming that the assembly of eukaryotic RNA pol II is similar to that of the bacterial polymerase, as subunit dissociation experiments suggest (3), it has been proposed that RNA pol II assembly would start with the formation of the Rpb3 subassembly, followed by the docking of the Rpb2 subassembly and finally the binding of the Rpb1 subassembly (4). The assembly process requires the participation of proteins that are not components of the mature enzyme. Several proteins that interact transiently with RNA pol II with a putative role as assembly factors have been identified. Thus, multiple interactions between GPN1/RPAP4 (Npa3p in yeast) and RNA pol II subunits in the soluble fraction of human cell extracts have been identified by performing protein affinity purification coupled to mass spectrometry (AP-MS) (5). GPN1 is a cytoplasmic-nuclear shuttling GTPase (5, 6) that associates with RNA pol II in a GTP-dependent manner (7). The involvement of GPN1 and its *Saccharomyces cerevisiae* homolog, Npa3p, in the nuclear import of RNA pol II has been confirmed by other reports (7, 8). Using MS-based quantitative proteomics on human cell extracts, a cytoplasmic RNA pol II intermediate containing the Rpb1p and Rpb8p subunits associated with the R2TP/prefoldin-like complex has been detected (9). The R2TP complex was identified in a set of high-throughput physical and genetic interaction screens of the Hsp90 chaperone in yeast (10), and a homologous complex was later described in humans (11, 12).

Another protein involved in the nuclear import of RNA pol II is Iwr1p. This protein was identified in a genetic screen for sup-

pressors of the growth defect caused by depletion of the transcription repressor NC2 (13, 14) and in high-throughput MS screens of yeast as a protein that interacts with RNA pol II (15, 16). Deletion of *IWR1* has major effects on the cell transcription profile (14, 17), although Iwr1p has not been associated with RNA pol II when this enzyme is recruited to the promoter of active genes (14). In a recent report, Czeko et al. showed that Iwr1p binds to the active-center cleft formed by the two largest RNA pol II subunits (17). This binding pocket occurs only in mature polymerase, suggesting that Iwr1p binding is restricted to the completely assembled polymerase. Bound to RNA pol II, Iwr1p uses its nuclear localization signal (NLS) to direct the RNA pol II nuclear import via the classical importin α-dependent pathway. In the nucleus, Iwr1p is displaced from the active-center cleft of RNA pol II during transcription initiation complex formation and is exported to the cytoplasm using a nuclear export sequence in an Xpo1p-dependent manner (17).

Here we show that another gene identified as a suppressor of NC2 defects, *YMR185w*, encodes a protein that is structurally related to karyopherins and that is required for the nuclear localization of RNA pol II. We have renamed the *YMR185w* open reading frame *RTP1* (required for the nuclear transport of RNA pol II). The role of Rtp1p in the nuclear import of RNA pol II does not depend on Iwr1p because this protein can be imported into the nucleus in the absence of Rtp1p. Rtp1p physically interacts with

components of the R2TP complex and with several RNA pol II subunits. The pattern of interactions suggests a role for Rtp1p in facilitating the starting interaction between subassemblies Rpb2 and Rpb3 and then the interaction of the resulting complex with the Rpb1 subassembly. Besides, Rtp1p interacts with phenylalanine-glycine (FG)-containing nucleoporins *in vivo* and *in vitro*, suggesting that Rtp1p can also participate in the transport of RNA pol II through the nuclear pore complex (NPC).

MATERIALS AND METHODS

Strains, plasmids, and genetic methods. All of the strains used in this study are listed in Table S1 in the supplemental material. Standard genetic analysis and transformation methods were used. For the growth assays, yeast cultures were diluted to the same optical density at 600 nm and serial dilutions (1:10) were spotted onto YPD (2% dextrose, 1% yeast extract, 2% peptone) or YPGal (2% galactose, 1% yeast extract, 2% peptone). Doxycycline was used at a concentration of 10 mg/liter. The wild-type promoter was replaced with the *GAL10* promoter (including three copies of the hemagglutinin [HA] epitope), nonessential genes were deleted by substituting the coding sequence for the *his5* or the *kan^r* marker, and HA or green fluorescent protein (GFP) tags were added by using a PCR-based method as previously described (18). C-terminal tandem affinity purification (TAP) tags were added as described previously (19). Replacement of the wild-type promoter with the *tetO* promoter was performed as previously described (20). We were unable to transform the haploid Δ*rtp1* mutant strains. In order to introduce genomic changes into a Δ*rtp1* mutant background, the heterozygous Δ*rtp1/RTP1* diploid was transformed and sporulated to obtain the strain with the desired genotype. The genetic screen to isolate the suppressors of NC2 has been previously described (13).

In order to construct ptetO-IWR1-ΔNES-GFP, a NotI-PstI PCR fragment from pIWR1-ΔNES-GFP (14) was ligated into the NotI-PstI sites of the pCM189 vector (20). For the pGST-Nup100 construct, PCR was used to create a BglII site upstream and a EcoRV site downstream in a fragment between positions 4 and 1740 of the *NUP100* open reading frame. This fragment was inserted between the BamHI and SmaI sites of pGEX-3X (GE Healthcare). Similarly, PCR was used to obtain a BglII-EcoRV restriction fragment including the *NUP116* open reading frame between positions 4 and 2160. This fragment was inserted into the pGEX-3X polylinker to obtain the pGST-Nup116 construct. For the His$_6$-RTP1 construct, PCR was used to obtain a XhoI-PstI restriction fragment, including the *RTP1* open reading frame. This fragment was inserted into the XhoI-PstI sites of the pRSET-A plasmid (Life Technologies) to obtain the pRSET-RTP1 plasmid. To construct pBTM116-RTP1, a SmaI-PstI fragment was inserted into the BamHI (filled with Klenow fragment)-PstI sites of pBTM116. To construct pGAD-NUP100, a BamHI-PstI restriction fragment from pGST-Nup100 was cloned into the BamHI-PstI sites of pGAD-C1 (21). To construct pGAD-NUP116, an MfeI-NsiI fragment from pGST-Nup116 was cloned into the EcoRI-PstI sites of pGAD-C2 (21). YEp-Rpb2t has been previously described (13). The YEp-Rpb2t-TAP plasmid was made by introducing the TAP tag into the EcoRI site of *RPB2* in plasmid YEp-Rpb2t. To construct plasmid pRTP1-GFP, genomic DNA from the strain containing the *RTP1::GFP::Kan^r* allele was digested with SbfI and KasI and ligated into the YCplac33 vector. Plasmids with the right insert were selected in LB plates containing ampicillin and kanamycin.

Protein structure modeling. Rtp1p models were obtained from the I-TASSER server (http://zhanglab.ccmb.med.umich.edu/I-TASSER/). The structural homologs of Rtp1p were searched for with I-TASSER and PSIPRED (http://bioinf.cs.ucl.ac.uk/psipred/). The structural and functional analogs of Rtp1p were searched for with COFACTOR (http://zhanglab.ccmb.med.umich.edu/COFACTOR/). Protein structure figures were created with PyMOL (http://www.pymol.org/).

Fluorescence microscopy. Yeast cells grown to the early exponential phase were used for fluorescence microscopy. DAPI (4′,6-diamidino-2-

phenylindole) staining of 4% (wt/vol) paraformaldehyde-fixed cells was performed with 2.5 μg/ml (wild-type cells) or 7.5 μg/ml (Δ*iwr1* and Δ*rtp1* mutants) DAPI in phosphate-buffered saline (PBS) for 30 min, and the cells were washed three times with PBS to visualize GFP fusion proteins. Aliquots (1.2 μl) of the cultures were put onto microscope slides and covered with coverslips (18 by 18 mm). Cells were visualized using a Zeiss Axioskop II fluorescence microscope. Images were scanned with a SPOT digital camera (Diagnostic Instruments, Inc.). A quantitative estimation of the intensities of the nuclear and cytosolic signals was achieved by determining the ratio of the average pixel intensity in the nuclear region of the cell to that in the cytosolic region in at least 30 cells from three independent experiments with the AxioVision v4.7 software (Zeiss Inc.). Yeast immunofluorescence was carried out as previously described (22).

Yeast two-hybrid analysis. Yeast strain EGY40, containing the *lacZ* reporter plasmid pSH18-34 and the LexA-Rtp1p-expressing plasmid pBTM116-RTP1, was cotransformed with pGAD-NUP100, pGAD-NUP116, or the empty pGAD-C2 vector (21). Transformed cells were grown on synthetic complete medium lacking Leu-Trp-Ura to assay β-galactosidase activity as previously described (23).

***In vitro* pulldown assay.** The expression and purification of the glutathione *S*-transferase (GST) fusion proteins were performed as previously described (24). The *in vitro* binding assays were carried out as previously described (25). Immobilized GST fusion proteins (normalized to contain the same amount of beads) were incubated for 1 h at 4°C with the Ni^{2+} affinity chromatography-purified His$_6$-Rtp1p protein. Beads were extensively washed, resuspended in 2× Laemmli sample buffer, and analyzed on 10% polyacrylamide gels. Gels were stained with Coomassie blue to visualize the GST proteins. His$_6$-Rtp1p was detected by Western blotting using the anti-Xpress antibody (Life Technologies).

Immunoprecipitation. For the immunoprecipitation of HA- and TAP-tagged proteins, whole-cell extracts were prepared from yeast strains in lysis buffer containing 20 mM HEPES (pH 7.6), 150 mM NaCl, 5 mM MgCl$_2$, 10% glycerol, and protease inhibitors (Complete; Roche). A total of 6 mg of extract was incubated with 30 μl of HA-agarose (Roche) or 100 μl of IgG-Sepharose (GE Heathcare) and rotated at 4°C for 4 h. Beads were washed four times with 400 μl of lysis buffer. Bound proteins were eluted by incubation at 95°C for 5 min in 2× Laemmli sample buffer.

Tandem affinity purification and mass spectrometric analysis. Purification of Rtp1-TAP was performed as described previously (26). Rtp1-TAP and associated proteins were recovered from cell extracts by affinity selection on an IgG matrix. After washing, the *Tobacco etch virus* (TEV) protease was added to release the bound material. The eluate was incubated with calmodulin-coated beads in the presence of calcium. After washing, the bound material was released by incubation with EGTA. The eluate was analyzed by multidimensional protein identification technology (MudPIT) by mass spectrometry (27) or trichloroacetic acid precipitated and analyzed by Western blotting.

Western blot analysis. The proteins eluted from immunoprecipitated complexes or the total protein extracts prepared by alkaline lysis of exponentially growing yeast (28) were separated by 8% SDS-PAGE. HA-tagged proteins were detected with the 3F10 monoclonal anti-HA antibody (Roche), TAP-tagged proteins were detected with anti-PAP antibody (Sigma), Rpb1p was detected with the 8WG16 monoclonal antibody (Covance), and Rpb3p was detected with the anti-Rpb3p monoclonal antibody (NeoClone). Chemiluminescence was visualized (ECL Advanced; GE Healthcare) according to the manufacturer's instructions.

RESULTS

YMR185w/RTP1 mutations suppress the depletion of transcriptional repressor NC2. In order to identify mutations that suppress the requirement for NC2, we used a yeast strain in which the genes encoding the two NC2 components (*YDR1* and *BUR6*) are under the control of the *GAL10* promoter. Transposon insertion mutants were generated in this strain by using a yeast genomic library mutagenized by the insertion of an *mTn3-lacZ/LEU2*
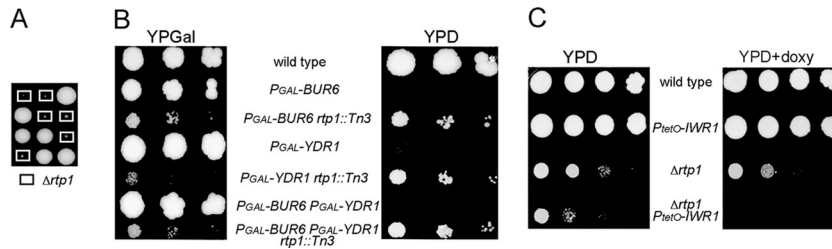
FIG 1 *RTP1* is a nonessential gene whose deletion suppresses the depletion of NC2 components Bur6p and Ydr1p. (A) Heterozygous diploid Δ*rtp1*::*Kan^r*/*RTP1* was sporulated and segregants were incubated in a YPD plate for 8 days at 25°C. Segregants carrying the Δ*rtp1*::*Kan^r* deletion are indicated by rectangles. (B) The *rtp1* mutation was combined with the *P_GAL10*-*BUR6* and/or *P_GAL10*-*YDR1* alleles, and the wild-type (FY86) and mutant cells were spotted onto YPGal or YPD plates and incubated for 8 days. (C) Genetic interactions between *rtp1* and *iwr1* mutations. Wild-type (FY86) and mutant strains were spotted onto YPD plates or YPD plates supplemented with 10 mg/liter doxycycline (doxy) and incubated for 6 days at 30°C.

transposon (29). Suppressor mutants were selected for the ability to grow on dextrose-containing plates at room temperature, and transposon insertion sites were determined. We isolated three independent clones in which transposon insertions were mapped at different locations in the *YMR185w*/*RTP1* open reading frame (nucleotide positions 511, 923, and 1173 from the ATG codon). Thus, suppression was most likely to be the consequence of a complete loss of the Rtp1p function, as the insertion at 511 nucleotides from the ATG codon results in the production of an N-terminal 170-amino-acid fragment of the 982-amino-acid *RTP1* open reading frame. Reports on whether the *RTP1* null mutant is viable or not have conflicted (30, 31). Therefore, we analyzed the viability of the *rtp1* null mutant in our background by sporulating a heterozygous diploid. Although the four spores were viable, the segregants carrying a complete deletion of *RTP1* exhibited extremely impaired growth (Fig. 1A). As expected, mutation of *RTP1* suppressed the growth defects caused by the depletion of either or both NC2 components (Fig. 1B).

In addition to some components of the basal transcriptional machinery, our screen for suppressors of the NC2 function identified *IWR1* and *RTP1* (13, 14; this report). To investigate whether *RTP1* and *IWR1* are genetically related, we constructed a yeast strain carrying a deletion of *RTP1* and the *IWR1* gene under the control of the repressible *tetO* promoter. As observed in Fig. 1C, depletion of Iwr1p by addition of doxycycline in the absence of Rtp1p abolished cell growth.

Structural analysis and cellular localization of Rtp1p. Two of the several Rtp1p models obtained with I-TASSER gave C score values of −1.30 and −1.31, which were above the conventional −1.5 confidence cutoff value (32). The protein structures used as templates to build these models were human importin b (Protein Data Bank [PDB] ID 1QGK) (33) and transportin 1 (PDB ID 2Z5K) (34). A number of structures corresponding to human and yeast proteins with significant structural homology to Rtp1p were detected by I-TASSER and PSIPRED. The common feature of all of these proteins was the characteristic HEAT repeat architecture of the karyopherin-β (Kapβ) family (35). The sequence identity of Rtp1p with homologous proteins from higher eukaryotes was too low to yield meaningful results with sequence comparison programs. The structural and phylogenetic relationship can be consistently established by using algorithms that compare secondary and tertiary structures. By combining both approaches, we concluded that the protein encoded by the *TMCO7* gene is the closest human relative to Rtp1p.

We analyzed the cellular localization of Rtp1p *in vivo* by using

an Rtp1-GFP fusion (expressed under the control of the *RTP1* promoter) (Fig. 2A) and by indirect immunofluorescence utilizing an HA-Rtp1p fusion (expressed under the control of the strong *GAL10* promoter) (Fig. 2B). In both cases, Rtp1p was observed throughout the cell. We did not detect any significant change in the cellular localization of Rtp1p through the deletion of
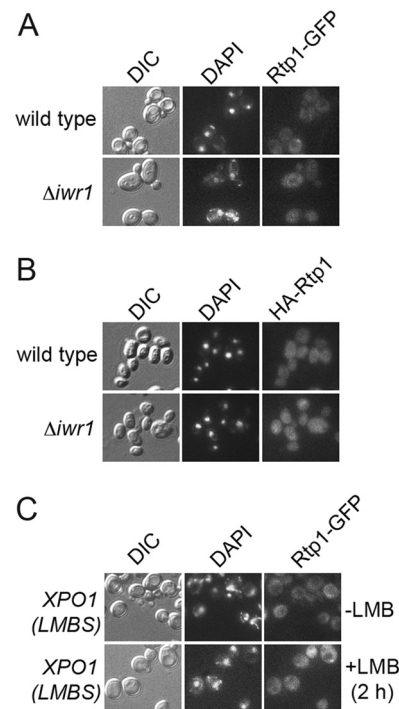
FIG 2 Cellular localization of Rtp1p. (A) The wild type (FY86) and a Δ*iwr1* (*iwr1-Δ1*) mutant expressing an Rtp1-GFP fusion were grown to the mid-exponential phase in YPD medium at 30°C. Cells were observed by differential interference contrast (DIC) and fluorescence microscopy for GFP. The position of the nuclei was visualized with DAPI. (B) Immunofluorescent localization of HA-Rtp1p. The wild type (FY86) and a Δ*iwr1* (*iwr1-Δ1*) mutant expressing *P_GAL10*-*RTP1*, in which the wild-type promoter of *RTP1* was replaced with the *GAL10* promoter, including three copies of the HA epitope, were processed for immunofluorescence microscopy with the 3F10 anti-HA antibody and Cy3-conjugated goat anti-mouse secondary antibody and stained with DAPI to detect DNA. (C) The LMB-sensitive (LMBS) *XPO1* mutant strain (CCY001) expressing an Rtp1-GFP fusion was grown to the mid-exponential phase in YPD medium at 30°C. Cells were incubated for 2 h in either the absence (−LMB) or the presence (+LMB) of 100 ng/ml LMB. Cells, Rtp1-GFP, and nuclei were visualized as described for panel A.

A

B
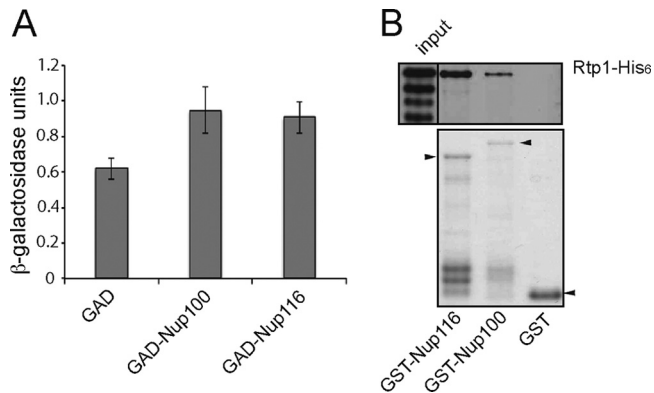
FIG 3 *In vivo* (two-hybrid) and *in vitro* (pulldown) interactions between Rtp1p and the GLFG region of Nup100p and Nup116p. (A) β-Galactosidase activity resulting from the two-hybrid interactions between Rtp1p-GBD and Nup100p-GAD and Nup116p-GAD. Assays were conducted in triplicate with yeast transformants containing the respective plasmids along with pSH18-34. Results obtained with pGAD-NUP100 and pGAD-NUP116 differed significantly from those obtained with pGAD, as determined by the two-tailed Student *t* test for groups of unequal variance ($P < 0.01$). (B) Bacterially expressed GST, GST-(GLFG)-Nup100, and GST-(GLFG)-Nup116 were immobilized on glutathione-agarose beads. Arrowheads indicate full-length (GLFG)-Nup100 and (GLFG)-Nup116 proteins. Recombinant purified Rtp1p-His$_6$ was added, and the bound fraction was eluted. A total of 4% of the Rtp1p-His$_6$ (input) and eluted fractions were resolved by SDS-PAGE and detected by Western blotting with the Xpress antibody.

IWR1 (Fig. 2A and B). To check whether Rtp1p shuttles between the nucleus and the cytoplasm in an Xpo1p-dependent manner, we examined the localization of Rtp1-GFP in an *XPO1T539C* mutant strain. In this strain, leptomycin B (LMB) addition inhibits Xpo1p-mediated transport (36). The cellular distribution of Rtp1-GFP was not affected by LMB addition, even with long incubations times (Fig. 2C).

Rtp1p interacts *in vivo* and *in vitro* with Nup100p and Nup116p. In *S. cerevisiae*, there are 14 known members of the Kapβ family. Besides the HEAT repeat architecture, these proteins have similar molecular masses (90 to 150 kDa) and isoelectric points (pI 4.0 to 5.0) (reviewed in reference 37). Rtp1p has a molecular mass of 113 kDa and an isoelectric point of 4.91 (*Saccharomyces* Genome Database).

Kapβ proteins bind weakly to the FG repeats of NPC nucleoporins and target Kapβ-cargo complexes to the NPC for translocation (37). To investigate whether Rpt1p interacts *in vivo* with the FG-containing nucleoporins, we used the two-hybrid system by fusing full-length Rtp1p with the LexA DNA binding domain (LexA-Rtp1p), and the GLFG-containing region of Nup100p and Nup116p with the Gal4p transcription activation domain (GAD-Nup100p and GAD-Nup116p, respectively). Cotransformation of LexA-Rtp1p and GAD-Nup100p (or GAD-Nup116p) had a negative effect on cell growth (results not shown). However, a weak but significant interaction was observed *in vivo* between Rtp1p and the nucleoporins by measuring the induction of the *lacZ* reporter gene (Fig. 3A). To test whether the detected two-hybrid interaction between Rtp1p and the GLFG repeats of Nup100p and Nup116p was direct, we performed soluble binding assays with recombinant purified proteins. The *RTP1* open reading frame was cloned into the pRSET-A plasmid. The Rtp1p protein expressed by this plasmid includes a polyhistidine tag and the Xpress epitope in the N-terminal region for immunological detection. The levels

of the fusion protein expressed by this plasmid were too low to be detected by Coomassie staining, but it was detected by Western blotting with the Xpress antibody. Rtp1p was purified as a His$_6$ fusion protein by Ni-agarose chromatography and imidazole elution. The purified His$_6$-Rtp1p fraction contained the full-length protein (113 kDa) and smaller bands, likely corresponding to proteolytic products (input, Fig. 3B). The GLFG regions of Nup116p and Nup100p were purified as GST fusion proteins and immobilized on glutathione-Sepharose. His$_6$-Rtp1p was incubated with GST-Nup116p, GST-Nup100p, or GST (control). Bound fractions were separated and analyzed by Western blotting for the Xpress epitope. His$_6$-Rtp1p did not bind to GST alone (Fig. 3B). In contrast, the binding of the full-length His$_6$-Rtp1p (but not the smaller bands) was detected with both GST-Nup116p and GST-Nup100p, suggesting a direct association between Rtp1p and the GLFG regions of these proteins.

Kapβ family members also bind RanGTP preferentially in their N-terminal arches (37). Rtp1p was not identified in a homology search based on an alignment of the conserved N-terminal region of Kapβ proteins (38). Besides, we failed to identify Rtp1p among the proteins bound to functional yeast Ran (Gsp1p or Gsp2p) tagged with protein A (39) (results not shown).

The involvement of alternative pathways for importing RNA pol II has been suggested after the identification of the conserved GTPase RPAP4/GPN1/Npa3p as an RNA pol II nuclear import factor (5, 7, 8). However, we also failed to detect an interaction *in vivo* between Rtp1p and Npa3p (results not shown).

Rtp1p is required for nuclear import and physically interacts with RNA pol II. The predicted structure of the Rtp1p protein and its interactions with nucleoporins suggest a role for this protein in nucleocytoplasmic transport. Another gene identified in our screen, which is both genetically and phenotypically related to *RTP1*, *IWR1*, encodes a protein involved in the nuclear import of RNA pol II (17). These results prompted us to analyze the effect of *rtp1* deletion on the cellular localization of RNA pol II. First, we analyzed the distribution of the largest subunit of RNA pol II, Rpb1p, by introducing an Rpb1p-GFP fusion into the wild-type and Δ*rtp1* mutant strains. In the wild-type strain, Rpb1p was localized mainly in the nucleus, but it exhibited cytoplasmic localization in the mutant strain containing an *RTP1* deletion (Fig. 4A). This result was confirmed by *in situ* immunolocalization of Rpb1p using an 8W16G antibody that reacts against the Rpb1p carboxy-terminal domain repeats (results not shown).

Two major assembly intermediates of RNA pol II have been described: one containing Rpb1p and another containing Rpb2p (5, 9). To establish whether Rtp1p is also involved in the nuclear import of other RNA pol II subunits, we investigated the localization of Rpb2p in the Δ*rtp1* mutant. Similarly to Rpb1p, the mutation in *RTP1* caused the complete mislocalization of the second largest RNA pol II subunit, Rpb2p (Fig. 4B).

In order to analyze whether Rtp1p is required for the import of RNA pol I and RNA pol III, we constructed yeast strains carrying GFP fusion proteins for the largest subunits of RNA pol I (Rpa190p) and RNA pol III (Rpo31p). As observed in Fig. 4C, the subcellular localization of these subunits was unaffected in the *rtp1* mutant.

The above results indicate that Rtp1p is required for the nuclear import of RNA pol II, suggesting that the enzyme is a cargo of Rtp1p. Therefore, we investigated the interactions of Rtp1p with different RNA pol II subunits. We evaluated the interaction be-
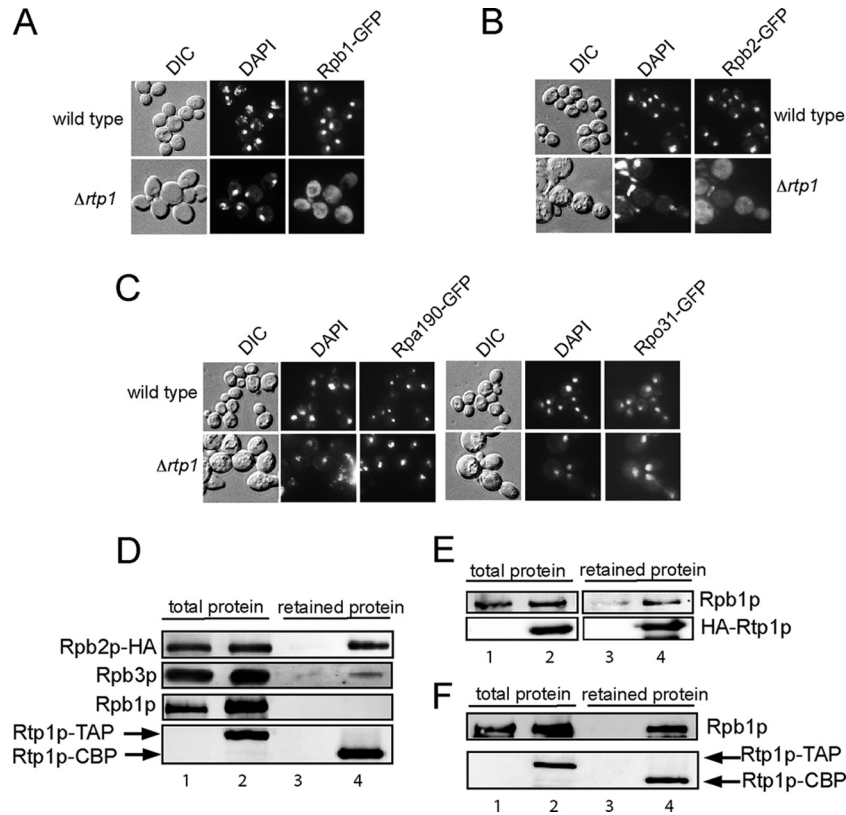
FIG 4 Rtp1p is required for the nuclear localization of RNA pol II and physically interacts with the RNA pol II subunits. The RNA pol II subunits (Rpb1p in panel A and Rpb2p in panel B) fused to GFP were expressed in the wild-type and Δ*rtp1* mutant strains. Yeast cells were grown in YPD at 30°C and harvested in the early exponential phase. Living cells were observed by differential interference contrast (DIC) and fluorescence microscopy for GFP. The position of the nuclei was visualized with DAPI. (C) The largest subunits of RNA pol I (Rpa190p) and RNA pol III (Rpo31p) expressed in the wild-type and the Δ*rtp1* mutant were observed as described in panel A. (D) Coimmunoprecipitation assays with endogenous TAP-tagged Rtp1p (lanes 2 and 4) and an untagged Rtp1p control strain (lanes 1 and 3). Both strains included a version of Rpb2p tagged at the C terminus with three copies of the HA epitope. TAP-tagged proteins were immunoprecipitated with IgG-Sepharose and eluted by TEV protease digestion. The resulting Rtp1p-CBP fusion protein was purified by calmodulin-Sepharose chromatography. Proteins in the extract (total proteins [lanes 1 and 2] or protein associated with Rtp1p, retained proteins [lanes 3 and 4]) were detected by immunoblotting with anti-TAP (Thermo Scientific) for Rtp1p-TAP, the 3F10 anti-HA antibody (GE Healthcare) for Rpb2p-HA, the 8WG16 antibody (Covance) for Rpb1p, or the anti-Rpb3p antibody (NeoClone) for Rpb3p. (E) Strain P_{GAL10}-*RTP1*, in which the wild-type promoter of *RTP1* was replaced with the *GAL10* promoter, including three copies of the HA epitope (lanes 2 and 4) and an untagged control strain (lanes 1 and 3), which were grown in YPGal to the early exponential phase. The Rtp1p-HA protein was immunoprecipitated with anti-HA Sepharose beads (GE Healthcare). Proteins in the extract (total proteins [lanes 1 and 2] or protein associated with Rtp1p, retained proteins [lanes 3 and 4]) were detected by immunoblotting with the 3F10 anti-HA antibody (GE Healthcare) for Rtp1p-HA or the 8WG16 antibody (Covance) for Rpb1p. (F) Endogenous TAP-tagged Rtp1p in the Δ*iwr1* mutant strain (lanes 2 and 4) and untagged Rtp1p in a Δ*iwr1* mutant as a control (lanes 1 and 3) were used for the coimmunoprecipitation assay as described for panel D.

tween Rtp1p and the two largest RNA pol II subunits and Rpb3p using a strain expressing 3 × HA-tagged Rpb2p and TAP-tagged Rtp1p. The Rtp1p complex purified by tandem chromatography and proteolytic cleavage with TEV protease included Rpb2p-HA and, to a lesser extent, Rpb3p (Fig. 4D). None of these subunits was recovered when a strain containing Rpb2p-HA, but not Rtp1p-TAP, was used as a negative control. We were unable to detect the Rpb1p subunit in the retained Rtp1p-TAP fraction (Fig. 4D), but an interaction between Rtp1p and Rpb1p was observed when HA-tagged Rtp1p was overexpressed using the strong *GAL10* promoter (Fig. 4E). This result suggests that the interaction between Rtp1p and Rpb1p was too weak or too transient to be detected using wild-type levels of proteins. If this were the case, it would be possible to increase the interaction between Rtp1p and Rpb1p by interfering with the nuclear import of fully assembled RNA pol II, as occurs in the absence of Iwr1p (17). Accordingly, the TAP purification of Rtp1p in the Δ*iwr1* strain permitted the

detection of Rpb1p in the immunoprecipitated complex with wild-type levels of proteins (Fig. 4F).

Iwr1p can be imported into the nucleus in the absence of Rtp1p. Based on the presence of a bipartite NLS in Iwr1p and on the *in vitro* binding of Iwr1p with karyopherin Kap60p, Czeko et al. reported that Iwr1p directs RNA pol II import via Kap60p/Kap95p (17). We confirmed this result by using GFP-tagged strains in which *KAP60* and *KAP95* were expressed under the control of the *GAL10* promoter with Iwr1p carrying a deletion in its nuclear export signal [Iwr1(ΔNES)-GFP]. This protein was expressed by using the strong and regulable *tetO* promoter. Cytoplasmic accumulation of Iwr1(ΔNES)-GFP was observed after a 5-h incubation of the P_{GAL10}-*KAP60* and P_{GAL10}-*KAP95* mutant strains in glucose-containing medium; after 7 h, fluorescence was observed throughout the cell (Fig. 5A). As predicted by the model suggested by Czeko et al., depletion of Kap60p or Kap95p also caused the cytoplasmic accumulation of the Rpb1-GFP fusion protein, which was visible after 9 h of incu-
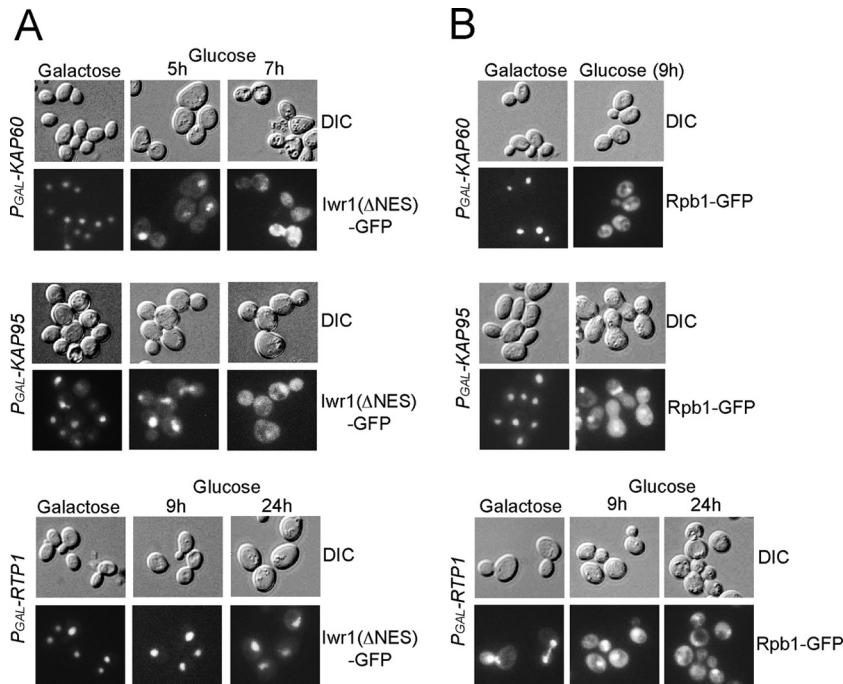
FIG 5 Localization of Iwr1p(ΔNES) (A) and Rpb1p (B) in cells depleted of Rtp1p (P_{GAL10}-RTP1) or the components of the α-importin pathway (P_{GAL10}-KAP60 and P_{GAL10}-KAP95). Iwr1p(ΔNES) and Rpb1p fused to GFP were expressed in cells in which the promoter of *RTP1*, *KAP60*, or *KAP95* was replaced with the regulatable *GAL10* promoter. Cells were grown in YPGal (Galactose), harvested in the early exponential phase, and transferred to YPD (Glucose) for the indicated times. Living cells were observed by differential interference contrast (DIC) and fluorescence microscopy.

bation in glucose; nonetheless, complete loss of the nuclear signal required longer incubation times (results not shown).

We also constructed a mutant strain in which *RTP1* was expressed under the control of the *GAL10* promoter. As expected, growth of the P_{GAL10}-*RTP1* strain in glucose was impaired, although Rtp1p-depleted cells still grew better than the Δ*rtp1* null strain (results not shown). Depletion of Rtp1p caused the cytoplasmic accumulation of the Rpb1p-GFP protein (Fig. 5B). Unlike the *kap60* and *kap95* mutants, however, the impaired localization of Rpb1p in the *rtp1* mutant did not correspond to the cytoplasmic accumulation of Iwr1(ΔNES)-GFP, as this protein was observed in the nucleus even after a 24-h incubation in glucose (Fig. 5A). The nuclear localization of Iwr1(ΔNES)-GFP was not a consequence of the residual expression of the P_{GAL10}-*RTP1* promoter in glucose because Iwr1(ΔNES)-GFP was also detected in the nucleus of the Δ*rtp1* null strain (results not shown). These results suggest that Iwr1p, and likely other proteins containing a classical NLS, can be imported into the nucleus in the absence of Rtp1p. Once again, Rtp1p was not required for the nuclear import of the TATA binding protein (Tbp1p) (results not shown), which is mediated by Kap114p (40).

In order to determine whether other karyopherins participate in the nuclear import of RNA pol II, we also analyzed the effect of the mutation in a variety of karyopherin genes on the localization of Rpb1p. In all of the mutants tested (Δ*kap108*, Δ*kap114*, Δ*kap120*, Δ*kap122*, Δ*kap123*, and P_{tetO}-*PSE1* mutants in doxycycline-containing medium), the localization of Rpb1p remained unchanged (results not shown).

Rtp1p interacts with components of the R2TP complex. In order to further characterize Rtp1p, we proceeded to identify the proteins that associate with Rtp1p by using AP-MS. We purified

Rtp1p-TAP and analyzed the enriched calmodulin eluate by using MudPIT to identify the polypeptide mixture present in our affinity purification. Our MudPIT analysis (Table 1) not only confirmed the interaction between Rtp1p and Rpb2p detected by coimmunoprecipitation (Fig. 4D) but revealed an interaction between Rtp1p and three of the four subunits of the R2TP complex (Rvb1p, Rvb2p, and Pih1p). The R2TP complex is involved in distinct cellular processes, including RNA pol II assembly (41). The interaction between Rtp1p and some of these proteins was corroborated by Western blotting (Fig. 6A and B). However, we failed to detect an interaction between Rtp1p and the fourth component of the R2TP complex not identified in our MudPIT analysis, Tah1p (result not shown).

In human cells, it has been suggested that the R2TP complex promotes the association of Rpb1p with the assembling polymerase (4, 9). A similar situation might occur in yeast since we detected an interaction between R2TP component Rvb2p and Rpb1p (Fig. 6C).

The involvement of the R2TP components in the nuclear im-

TABLE 1 Rtp1-TAP purification identify Rpb2p and R2TP components

Copurified protein	Description	No. of peptides	% coverage
Rtp1p	Uncharacterized protein YMR185w	26	30.5
Rpb2p	RNA pol II subunit	4	5
Rvb1p	RuvB-like protein 1	4	13
Rvb2p	RuvB-like protein 2	3	7
Pih1p	Protein interacting with Hsp90	1	3.5
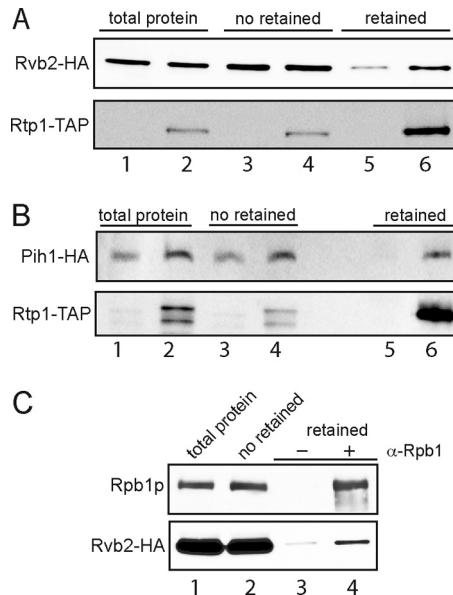
FIG 6 Rtp1p interacts with components of the R2TP complex. (A and B) Coimmunoprecipitation assays with endogenous TAP-tagged Rtp1p (lanes 2, 4, and 6) and the untagged Rtp1p control strain (lanes 1, 3, and 5). Both strains included a version of Rvb2p (A) or Pih1p (B) tagged at the C terminus with three copies of the HA epitope. TAP-tagged proteins were immunoprecipitated with IgG-Sepharose. Rtp1p-TAP was detected by immunoblotting with anti-PAP antibody (Sigma), while Rvb1p-HA and Pih1p-HA were detected with the 3F10 anti-HA antibody (GE Healthcare). In panel B, no sample was loaded in the lane between the nonretained and retained fractions. (C) Rvb2p interacts with Rpb1p. Rpb1p was immunoprecipitated with the 8WG16 (anti-Rpb1) antibody in a strain containing a version of Rvb2p tagged at the C terminus with three copies of the HA epitope. Proteins were detected with the 8WG16 (Rpb1p) and 3F10 anti-HA (Rvb2p) antibodies.

port of RNA pol II was studied by analyzing the localization of the two largest subunits, Rpb1p and Rpb2p, by using GFP-tagged proteins in strains carrying deletions of *TAH1* and *PIH1* or repressing the essential *RVB2* gene under the control of the P_{tetO} promoter in the presence of doxycycline. A strain carrying *RVB1* under the control of the P_{tetO} promoter did not show any detectable growth defect in the presence of doxycycline and was not further used. Depletion of Rvb2p and deletion of *PIH1* slightly increased the cytoplasmic levels of Rpb1-GFP and Rpb2-GFP (Fig. 7). However, we observed no effect on the distribution of any of the RNA pol II subunits we analyzed upon the deletion of *TAH1* (Fig. 7).

Mislocalization of Rpb2-GFP caused by the expression of Rpb2tp, a truncated form of Rpb2p, can be suppressed by the overexpression of Rtp1p. The interaction of Rtp1p with components of the R2TP complex and the recovery of RNA pol II subunits in nonstoichiometric amounts in immunoprecipitated Rtp1p-TAP (Fig. 4D and E) may be indicative of a role for Rtp1p in RNA pol II biogenesis. The preeminent interaction with Rpb2p, and to a lesser extent with Rpb3p, is in agreement with a role for Rtp1p in facilitating the interaction of Rpb2p with the Rpb3 subassembly. This function is also consistent with the observation that the overexpression of the *RPB2* gene partially alleviates the requirement of Rtp1p for cell growth (result not shown). The interaction between Rtp1p and Rpb2p prompted us to revise the effect that the expression of a truncated allele of *RPB2* (named *rpb2t*) could have on RNA pol II localization. The expression of

Rpb2tp, from a 2μm-based plasmid, as occurs with the deletion of genes *RTP1* and *IWR1*, suppresses the growth defects caused by the depletion of NC2 components (13). We hypothesized that the suppressing effect of the truncated Rpb2p subunit could be caused by an impairment of RNA pol II biogenesis through the squelching of Rtp1p. To test this hypothesis, we first analyzed the effect of Rpb2tp expression on the cellular localization of RNA pol II. Figure 8A and B show that the presence of a multicopy plasmid containing the truncated *rpb2t* allele (YEp-Rpb2t) increases the cytosolic signal of Rpb2-GFP and, to a lesser extent, Rpb1-GFP. Next, we checked whether the effect of Rpb2tp could be reversed by overexpressing Rtp1p. As our hypothesis predicted, the overexpression of *RTP1* under the control of the *GAL10* promoter rescues the Rpb2-GFP nuclear localization defect in YEp-Rpb2t transformants (Fig. 8C and D).

Rtp1p physically interacts *in vivo* with the N-terminal region of Rpb2p. Suppression of the *rpb2t*-induced mislocalization of RNA pol II by *RTP1* overexpression suggests a physical interaction between the two proteins. In order to determine whether Rtp1p and Rpb2tp interact, we used a strain expressing 3 × HA-tagged Rtp1p and TAP-tagged Rpb2tp. HA-Rtp1p was recovered in the immunoprecipitate, but not when a strain containing HA-Rtp1p, and not Rpb2tp-TAP, was used as a negative control (Fig. 8E). The truncated *RPB2* allele contains the coding sequence for the first 379 amino acids of a total length of 1,224 residues for Rpb2p (13). Rpb3p was not detected in the Rpb2t-TAP complex (Fig. 8E), suggesting that the interaction between Rtp1p and Rpb2p may occur without Rpb3 subassembly binding.

Depletion of Rpb2p prevents the nuclear import of RNA pol II. Depletion of any RNA pol II subunit from human cells results in an accumulation of Rpb1p in the cytoplasm, suggesting that the cytoplasmic assembly of RNA pol II occurs prior to nuclear import (9). Our results suggest a similar situation in yeast, where the defective assembly of the Rpb2 subcomplex in the *rtp1* mutant can prevent the nuclear import of other subunits, like Rpb1p. In order to check whether the absence of Rpb2p causes the mislocalization of Rpb1p, we used a strain in which the promoter of *RPB2* was substituted for the repressible *tetO* promoter. The localization of Rpb1p was analyzed in both the absence and the presence of doxycycline. Figure 9 shows that the depletion of Rpb2p resulted in the mislocalization of Rpb1p; analogously, the depletion of Rpb1p resulted in the mislocalization of Rpb2p (Fig. 9).

DISCUSSION

In the present study, we identified a previously uncharacterized protein, Rtp1p, as a new component of the RNA pol II biogenesis machinery. Rtp1p is phenotypically related to Iwr1p, a protein whose depletion leads to RNA pol II import defects (17). Both mutations *iwr1* and *rtp1* have been identified as suppressors of the growth defect caused by the depletion of the NC2 transcriptional repressor (13). In addition, in our genetic screen, we isolated mutants in different components of the basic transcriptional machinery, including Mediator, TFIIH, and RNA pol II itself. Therefore, one main conclusion drawn from our results is that NC2 defects can be compensated by impairing RNA pol II holoenzyme activity in different ways, including a reduction in the amount of nuclear RNA pol II due to defective nuclear import.

The current model of RNA pol II nuclear import suggests the assembly of the enzyme in the cytoplasm before it is imported into the nucleus. This model is based mainly on the observation that
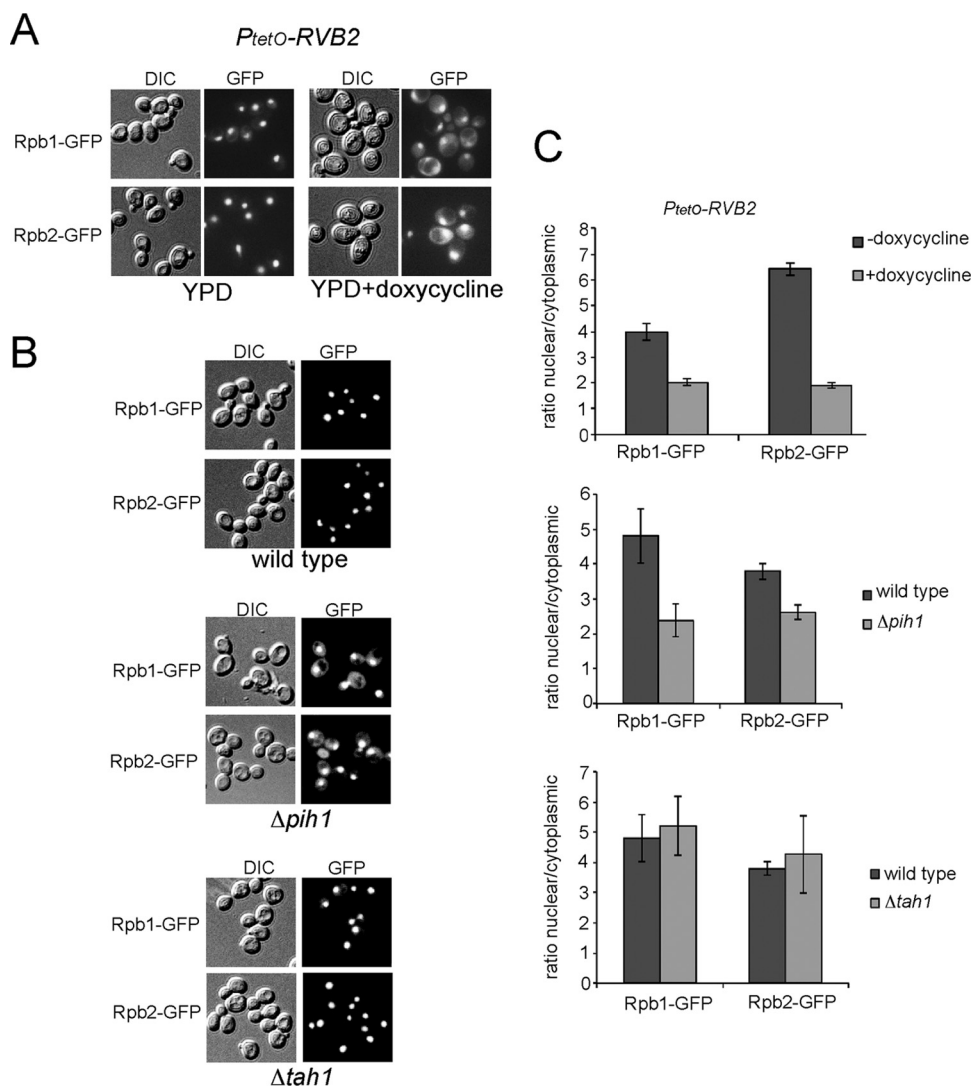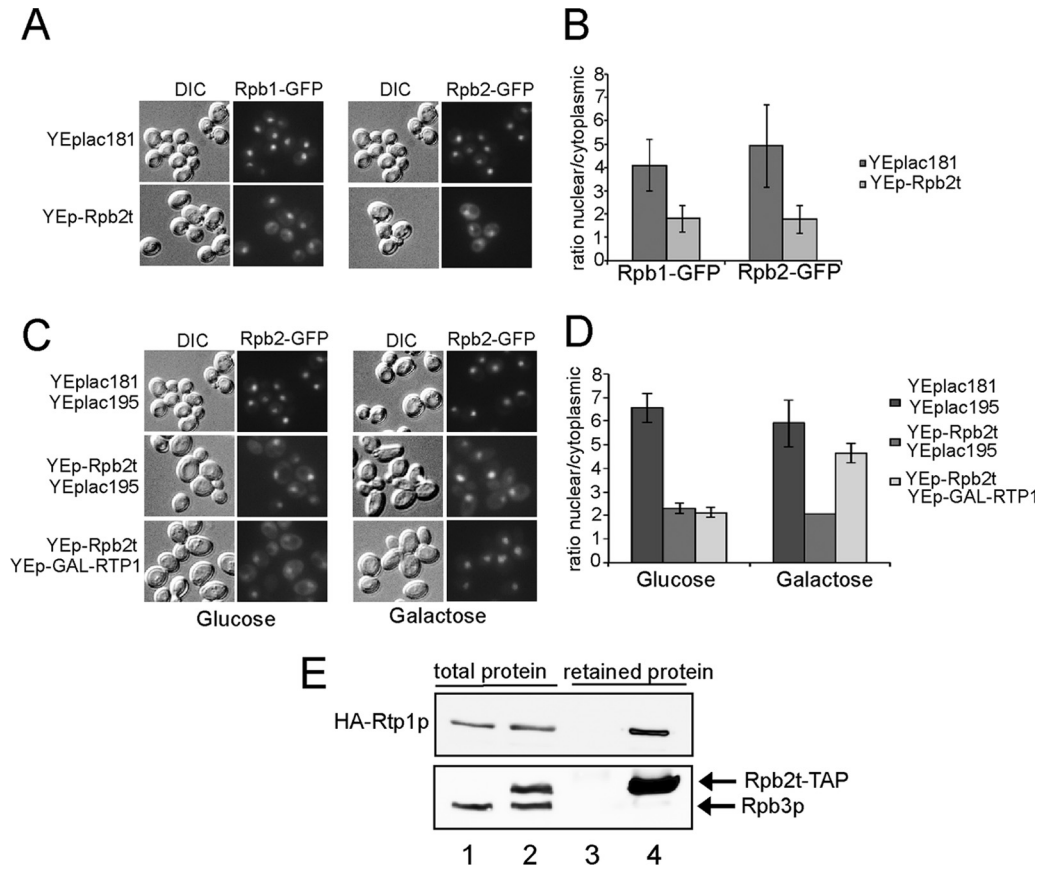
FIG 7 Nuclear localization of Rpb1p and Rpb2p in R2TP complex mutants. (A) The indicated subunits of RNA pol II fused to GFP were expressed in a strain in which the wild-type promoter of *RVB2* was replaced with the *tetO* promoter. Yeast cells were grown to the early exponential phase in YPD at 30°C and then transferred to YPD with or without 10 mg/liter doxycycline and incubated for 8 h at 30°C. (B) The indicated subunits of RNA pol II fused to GFP were expressed in the wild-type and Δ*pih1* and Δ*tah1* mutant strains. Yeast cells were grown in YPD at 30°C and harvested in the early exponential phase. Living cells were observed by differential interference contrast (DIC) and fluorescence microscopy for GFP. (C) Mean ratio of the quantified nuclear/cytoplasmic fluorescence ± the standard error of the mean ($n > 30$ cells) of the Rpb GFP fusion proteins shown in panels A and B. The graph represents the average nuclear/cytosolic intensity ratio derived from at least three independent cultures.

depletion of any RNA pol II subunit in human cells leads to the cytoplasmic accumulation of Rpb1p (12). Here we show in yeast that the nuclear import of one of the two large subunits (Rpb1p and Rpb2p) depends on the presence of the other, and vice versa (Fig. 9), suggesting that the nuclear import of yeast RNA pol II also requires a fully assembled enzyme in the cytoplasm. Once assembled, Iwr1p binds to RNA pol II and uses its NLS to direct the RNA pol II nuclear import through a karyopherin α-dependent pathway (17). Although the phenotypical consequences of the deletion of *IWR1* and *RTP1* are similar, our data suggest that the function of Rtp1p in nuclear transport is independent of the classical importin α pathway because Iwr1p can be imported into the nucleus in the absence of Rtp1p (Fig. 5). Besides, Iwr1p and Rtp1p display different patterns of interaction with the RNA pol II subunits. Interactions between Iwr1p and almost every RNA pol II subunit

have been detected in high-throughput MS screens (15, 16). In line with this, Czeko et al. have reported that Iwr1p binds to the active-center cleft of RNA pol II, which is formed by the association of subassemblies Rpb1 and Rpb2, the last event in RNA pol II assembly (17). Conversely, our MudPIT analysis of the proteins that interact with Rtp1p identified an interaction with Rpb2p but with no other RNA pol II subunits (Table 1). This interaction was confirmed by coimmunoprecipitation, which also revealed a weaker interaction with Rpb3p (Fig. 4D). We interpret the phenotype of the *rtp1* mutant and its pattern of interactions with RNA pol II subunits as being indicative of a role for Rtp1p in RNA pol II assembly (see Fig. 10). Absence of Rtp1p would block the assembly process, leading to a cytoplasmic accumulation of the RNA pol II subunits (Fig. 4A and B). The RNA pol II assembly process proposed by Wild and Cramer involves the formation of an interme-

FIG 8 (A) Localization of Rpb1p and Rpb2p in cells expressing Rpb2tp. Rpb1p and Rpb2p fused to GFP were expressed in cells transformed with plasmid YEp-Rpb2t or the empty vector YEplac181. (B) Mean ratio of the quantified nuclear/cytoplasmic fluorescence of the Rpb GFP fusion proteins shown in panel A. (C) Suppression of the Rpb2p mislocalization in cells expressing Rpb2tp by Rtp1p overexpression. (D) Mean ratio of the quantified nuclear/cytoplasmic fluorescence of the Rpb2-GFP fusion in the strains shown in panel C. Cells transformed with the indicated combination of plasmids were grown in YPD (Glucose) or YPGal (Galactose) and harvested in the early exponential phase. Living cells were observed by differential interference contrast (DIC) and fluorescence microscopy. The graph represents the average nuclear/cytosolic intensity ratio $\pm$ the standard error of the mean ($n > 30$ cells) derived from at least three independent cultures. (E) Rtp1p interacts with Rpb2tp. Coimmunoprecipitation assays with TAP-tagged Rpb2tp (lanes 2 and 4) and an untagged control strain (lanes 1 and 3). Both strains included a version of *RTP1* in which the wild-type promoter of *RTP1* was replaced with the *GAL10* promoter, including three copies of the HA epitope. TAP-tagged proteins were immunoprecipitated with IgG-Sepharose. The proteins in the extract (total proteins [lanes 1 and 2] or immuno-precipitated proteins [lanes 3 and 4]) were detected by immunoblotting with anti-TAP antibody (Thermo Scientific) for Rpb2tp-TAP, the 3F10 anti-HA antibody (GE Healthcare) for HA-Rtp1, or the anti-Rpb3p antibody (NeoClone) for Rpb3p.

diate containing subassemblies Rpb2 and Rpb3, followed by the binding of the Rpb1 subassembly (4). Our data indicate that Rtp1p interacts with Rpb2p. This interaction occurs through the N-terminal part of Rpb2p, as shown by the interaction between
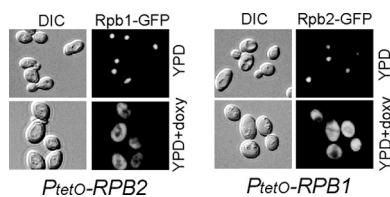
FIG 9 Cellular localization of RNA pol II in cells depleted of different RNA pol II subunits. The indicated subunits of RNA pol II (Rpb1p and Rpb2p) fused to GFP were expressed in strains in which the promoters of the genes encoding RNA pol II subunits Rpb1p and Rpb2p were replaced with the *tetO* promoter. Yeast cells were grown in YPD at 30°C, harvested in the early exponential phase, transferred to YPD either lacking (YPD) or containing 10 mg/liter doxycycline (YPD+doxy), and incubated for 8 h at 30°C. Living cells were observed by differential interference contrast (DIC) and fluorescence microscopy for GFP.

Rtp1p and a truncated version of Rpb2p, Rpb2tp (Fig. 8E). On the other hand, the absence of Rpb3p from the Rtp1p-Rpb2tp complex indicates that the interaction between Rtp1p and Rpb2p occurs before docking of the Rpb2 subassembly to the Rpb3 subassembly. We propose that Rtp1p works as an Rpb2p chaperone by facilitating the interaction between Rpb2p and the Rpb3 subassembly. Whether Rtp1p dissociates from the intermediate containing the Rpb2 and Rpb3 subassemblies or if it remains throughout the RNA pol II import process is a more controversial question. We were unable to observe an interaction between Rtp1p and Rpb1p when these proteins were expressed at the wild-type levels (Fig. 4D). This could imply that Rtp1p dissociates from Rpb2p after Rpb3 subassembly binding or that the interaction with the Rpb1 subassembly is too transient to be detected by co-immunoprecipitation. Our results support the notion that the interaction between Rtp1p and RNA pol II is maintained during the RNA pol II assembly process. Thus, an interaction between Rpb1p and Rtp1p was detected when Rtp1p was overexpressed (Fig. 4E), and the accumulation of RNA pol II competent complexes in the
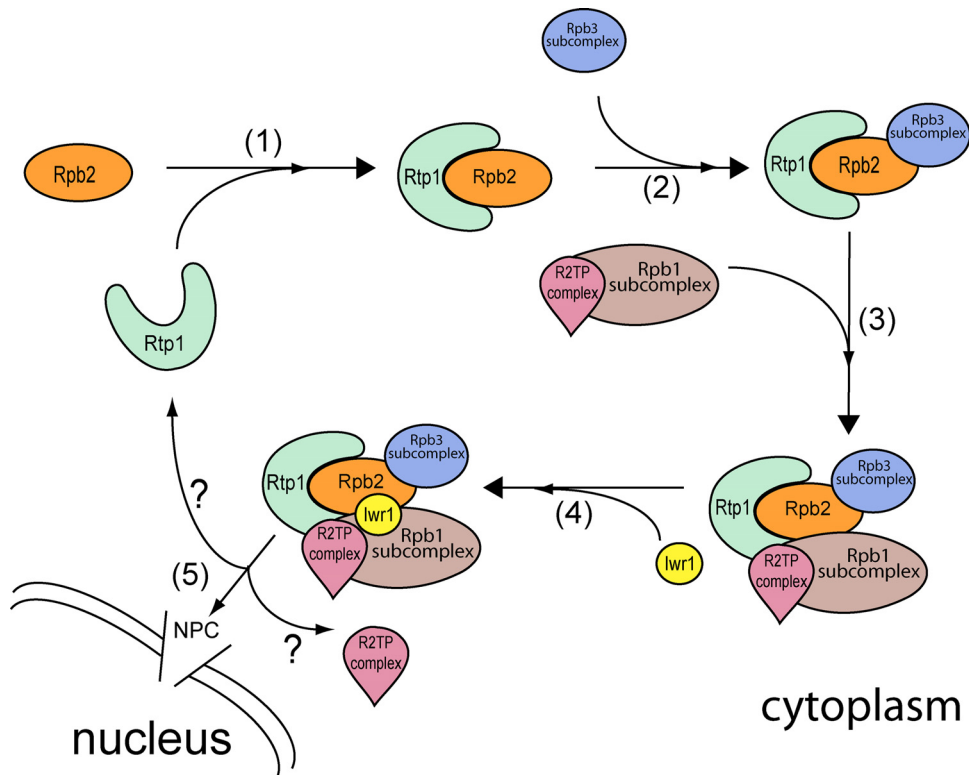
FIG 10 Model of Rtp1p participation in RNA pol II assembly. Rtp1p interacts with the N terminus of Rpb2p (step 1) and facilitates the interaction between the Rpb2 and Rpb3 subassembly complexes (step 2). Next, the two major assembly intermediates (still containing assembly factors like Rtp1p or the R2TP complex) join to form assembled RNA pol II (step 3). Iwr1p binds to the cleft of the fully assembled polymerase (step 4) and directs RNA pol II import through the NPC. It is unclear whether Rtp1p leaves the polymerase in the cytoplasm or remains in the complex by participating in the transport of RNA pol II through the NPC (step 5).

cytoplasm through the deletion of Iwr1p allowed the detection of Rpb1p in affinity-purified Rtp1-TAP complexes without protein overexpression being required (Fig. 4F). The presence of Rtp1p in the complex formed by the association of subassemblies Rpb1 and Rpb2/Rpb3 is also hinted at by the interaction of Rtp1p and the components of the R2TP complex (Table 1 and Fig. 6). Based on the analysis of RNA pol II assembly intermediaries in human cells, suggestions have been made that the R2TP complex participates in the recruitment of Hsp90 to the Rpb1 subassembly to promote the association of Rpb1p with the assembling polymerase (4, 9). We also detected an interaction between R2TP and Rpb1p (Fig. 6C). Thus, the interaction between Rtp1p and the components of the R2TP complex may be indicative of the presence of both assembly factors in the complex formed by the association of Rpb1 and Rpb2/Rpb3 subassemblies. To our knowledge, this is the first time that the R2TP complex has been related with RNA pol II biogenesis in yeast. R2TP has been identified in yeast as an Hsp90 co-chaperone, and it consists of four proteins: Rvb1, Rvb2p, Tah1, and Pih1p (10). Our analysis identified an interaction among Rtp1p and Rvb1, Rvb2p, and Pih1p (Table 1 and Fig. 6) but failed to detect an interaction with Tah1p. In the R2TP complex, Pih1p binds directly to the Rvb1p-Rvb2p complex but Tah1p does not (42). The failure to detect Tah1p in the Rtp1p complex may be due to experimental problems but might also indicate that a subcomplex containing Rvb1p-Rvb2p and Pih1p interacts with Rtp1p in yeast. The participation of this subcomplex in RNA pol II biogenesis is indicated by the partial defects in the cellular localization of

the large RNA pol II subunits observed in Rvb2p-depleted cells and in the Δ*pih1* mutant but not in the Δ*tah1* mutant. In any case, mutations in the components of the R2TP complex have only minor effects on the cellular distribution of the enzyme subunits, suggesting a secondary role for this complex in yeast RNA pol II biogenesis.

After the cytoplasmic assembly of RNA pol II, Rtp1p may either be displaced from RNA pol II or remain associated with the fully assembled enzyme by participating in transport through the NPC (Fig. 10). The structural analysis shows that Rtp1p possesses the characteristic molecular architecture of karyopherins. Besides, Rtp1p is able to interact with FG-containing nucleoporins *in vivo* and *in vitro* (Fig. 3). Therefore, it is tempting to speculate that Rtp1p can also act as an additional facilitator (together with Kap60p/Kap95p) in the RNA pol II import pathway. Nevertheless, we failed to detect an interaction between Rtp1p and Ran (Gsp1p and Gsp2p) or Npa3p, suggesting that the putative role of Rtp1p in nuclear import differs from that of the known karyopherins. Besides, unlike Iwr1p, Rtp1p does not shuttle between the nucleus and the cytoplasm in an Xpo1-dependent manner. Thus, further studies are required to establish whether Rtp1p plays a role in the transport of RNA pol II through the NPC.

ACKNOWLEDGMENTS

REFERENCES

1. Cramer P, Armache KJ, Baumli S, Benkert S, Brueckner F, Buchen C, Damsma GE, Dengl S, Geiger SR, Jasiak AJ, Jawhari A, Jennebach S, Kamenski T, Kettenberger H, Kuhn CD, Lehmann E, Leike K, Sydow JF, Vannini A. 2008. Structure of eukaryotic RNA polymerases. Annu. Rev. Biophys. 37:337–352.

2. Edwards AM, Kane CM, Young RA, Kornberg RD. 1991. Two dissociable subunits of yeast RNA polymerase II stimulate the initiation of transcription at a promoter in vitro. J. Biol. Chem. 266:71–75.

3. Kimura M, Ishiguro A, Ishihama A. 1997. RNA polymerase II subunits 2, 3, and 11 form a core subassembly with DNA binding activity. J. Biol. Chem. 272:25851–25855.

4. Wild T, Cramer P. 2012. Biogenesis of multisubunit RNA polymerases. Trends Biochem. Sci. 37:99–105.

5. Forget D, Lacombe AA, Cloutier P, Al-Khoury R, Bouchard A, Lavallee-Adam M, Faubert D, Jeronimo C, Blanchette M, Coulombe B. 2010. The protein interaction network of the human transcription machinery reveals a role for the conserved GTPase RPAP4/GPN1 and microtubule assembly in nuclear import and biogenesis of RNA polymerase II. Mol. Cell. Proteomics 9:2827–2839.

6. Reyes-Pardo H, Barbosa-Camacho AA, Pérez-Mejía AE, Lara-Chacón B, Salas-Estrada LA, Robledo-Rivera AY, Montero-Morán GM, Lara-González S, Calera MR, Sánchez-Olea R. 2012. A nuclear export sequence in GPN-loop GTPase 1, an essential protein for nuclear targeting of RNA polymerase II, is necessary and sufficient for nuclear export. Biochim. Biophys. Acta 1823:1756–1766.

7. Staresincic L, Walker J, Dirac-Svejstrup AB, Mitter R, Svejstrup JQ. 2011. GTP-dependent binding and nuclear transport of RNA polymerase II by Npa3 protein. J. Biol. Chem. 286:35553–35556.

8. Carré C, Shiekhattar R. 2011. Human GTPases associate with RNA polymerase II to mediate its nuclear import. Mol. Cell. Biol. 31:3953–3962.

9. Boulon S, Pradet-Balade B, Verheggen C, Molle D, Boireau S, Georgieva M, Azzag K, Robert MC, Ahmad Y, Neel H, Lamond AI, Bertrand E. 2010. HSP90 and its R2TP/Prefoldin-like cochaperone are involved in the cytoplasmic assembly of RNA polymerase II. Mol. Cell 39:912–924.

10. Zhao R, Davey M, Hsu YC, Kaplanek P, Tong A, Parsons AB, Krogan N, Cagney G, Mai D, Greenblatt J, Boone C, Emili A, Houry WA. 2005. Navigating the chaperone network: an integrative map of physical and genetic interactions mediated by the hsp90 chaperone. Cell 120:715–727.

11. Te J, Jia L, Rogers J, Miller A, Hartson SD. 2007. Novel subunits of the mammalian Hsp90 signal transduction chaperone. J. Proteome Res. 6:1963–1973.

12. Boulon S, Marmier-Gourrier N, Pradet-Balade B, Wurth L, Verheggen C, Jady BE, Rothe B, Pescia C, Robert MC, Kiss T, Bardoni B, Krol A, Branlant C, Allmang C, Bertrand E, Charpentier B. 2008. The Hsp90 chaperone controls the biogenesis of L7Ae RNPs through conserved machinery. J. Cell Biol. 180:579–595.

13. Peiró-Chova L, Estruch F. 2007. Specific defects in different transcription complexes compensate for the requirement of the negative cofactor 2 repressor in Saccharomyces cerevisiae. Genetics 176:125–138.

14. Peiró-Chova L, Estruch F. 2009. The yeast RNA polymerase II-associated factor Iwr1p is involved in the basal and regulated transcription of specific genes. J. Biol. Chem. 284:28958–28967.

15. Gavin AC, Aloy P, Grandi P, Krause R, Boesche M, Marzioch M, Rau C, Jensen LJ, Bastuck S, Dumpelfeld B, Edelmann A, Heurtier MA, Hoffman V, Hoefert C, Klein K, Hudak M, Michon AM, Schelder M, Schirle M, Remor M, Rudi T, Hooper S, Bauer A, Bouwmeester T, Casari G, Drewes G, Neubauer G, Rick JM, Kuster B, Bork P, Russell RB, Superti-Furga G. 2006. Proteome survey reveals modularity of the yeast cell machinery. Nature 440:631–636.

16. Krogan NJ, Cagney G, Yu H, Zhong G, Guo X, Ignatchenko A, Li J, Pu S, Datta N, Tikuisis AP, Punna T, Peregrin-Alvarez JM, Shales M, Zhang X, Davey M, Robinson MD, Paccanaro A, Bray JE, Sheung A,

Beattie B, Richards DP, Canadien V, Lalev A, Mena F, Wong P, Starostine A, Canete MM, Vlasblom J, Wu S, Orsi C, Collins SR, Chandran S, Haw R, Rilstone JJ, Gandi K, Thompson NJ, Musso G, St Onge P, Ghanny S, Lam MH, Butland G, Altaf-Ul AM, Kanaya S, Shilatifard A, O'Shea E, Weissman JS, Ingles CJ, Hughes TR, Parkinson J, Gerstein M, Wodak SJ, Emili A, Greenblatt JF. 2006. Global landscape of protein complexes in the yeast Saccharomyces cerevisiae. Nature 440:637–643.

17. Czeko E, Seizl M, Augsberger C, Mielke T, Cramer P. 2011. Iwr1 directs RNA polymerase II nuclear import. Mol. Cell 42:261–266.

18. Longtine MS, McKenzie A, III, Demarini DJ, Shah NG, Wach A, Brachat A, Philippsen P, Pringle JR. 1998. Additional modules for versatile and economical PCR-based gene deletion and modification in Saccharomyces cerevisiae. Yeast 14:953–961.

19. Puig O, Caspary F, Rigaut G, Rutz B, Bouveret E, Bragado-Nilsson E, Wilm M, Seraphin B. 2001. The tandem affinity purification (TAP) method: a general procedure of protein complex purification. Methods 24:218–229.

20. Garí E, Piedrafita L, Aldea M, Herrero E. 1997. A set of vectors with a tetracycline-regulatable promoter system for modulated gene expression in Saccharomyces cerevisiae. Yeast 13:837–848.

21. James P, Halladay J, Craig EA. 1996. Genomic libraries and a host strain designed for highly efficient two-hybrid selection in yeast. Genetics 144:1425–1436.

22. Juanes MA, Queralt E, Bano MC, Igual JC. 2007. Rot1 plays an antagonistic role to Clb2 in actin cytoskeleton dynamics throughout the cell cycle. J. Cell Sci. 120:2390–2401.

23. Ausubel FM, Brent R, Kingston RE, Moore PD, Seidman JG, Smith JA, Struhl K (ed). 1994. Current protocols in molecular biology. John Wiley & Sons, New York, NY.

24. Strahm Y, Fahrenkrog B, Zenklusen D, Rychner E, Kantor J, Rosbach M, Stutz F. 1999. The RNA export factor Gle1p is located on the cytoplasmic fibrils of the NPC and physically interacts with the FG-nucleoporin Rip1p, the DEAD-box protein Rat8p/Dbp5p and a new protein Ymr 255p. EMBO J. 18:5761–5777.

25. Estruch F, Hodge CA, Rodriguez-Navarro S, Cole CN. 2005. Physical and genetic interactions link the yeast protein Zds1p with mRNA nuclear export. J. Biol. Chem. 280:9691–9697.

26. Pascual-García P, Govind CK, Queralt E, Cuenca-Bono B, Llopis A, Chavez S, Hinnebusch AG, Rodriguez-Navarro S. 2008. Sus1 is recruited to coding regions and functions during transcription elongation in association with SAGA and TREX2. Genes Dev. 22:2811–2822.

27. Graumann J, Dunipace LA, Seol JH, McDonald WH, Yates JR, III, Wold BJ, Deshaies RJ. 2004. Applicability of tandem affinity purification MudPIT to pathway proteomics in yeast. Mol. Cell. Proteomics 3:226–237.

28. Soriano-Carot M, Bano MC, Igual JC. 2012. The yeast mitogen-activated protein kinase Slt2 is involved in the cellular response to genotoxic stress. Cell Div. 7:1. doi:10.1186/1747-1028-7-1.

29. Burns N, Grimwade B, Ross-Macdonald PB, Choi EY, Finberg K, Roeder GS, Snyder M. 1994. Large-scale analysis of gene expression, protein localization, and gene disruption in Saccharomyces cerevisiae. Genes Dev. 8:1087–1105.

30. Watanabe M, Watanabe D, Nogami S, Morishita S, Ohya Y. 2009. Comprehensive and quantitative analysis of yeast deletion mutants defective in apical and isotropic bud growth. Curr. Genet. 55:365–380.

31. Giaever G, Chu AM, Ni L, Connelly C, Riles L, Veronneau S, Dow S, Lucau-Danila A, Anderson K, Andre B, Arkin AP, Astromoff A, El-Bakkoury M, Bangham R, Benito R, Brachat S, Campanaro S, Curtiss M, Davis K, Deutschbauer A, Entian KD, Flaherty P, Foury F, Garfinkel DJ, Gerstein M, Gotte D, Guldener U, Hegemann JH, Hempel S, Herman Z, Jaramillo DF, Kelly DE, Kelly SL, Kotter P, LaBonte D, Lamb DC, Lan N, Liang H, Liao H, Liu L, Luo C, Lussier M, Mao R, Menard P, Ooi SL, Revuelta JL, Roberts CJ, Rose M, Ross-Macdonald P, Scherens B, Schimmack G, Shafer B, Shoemaker DD, Sookhai-Mahadeo S, Storms RK, Strathern JN, Valle G, Voet M, Volckaert G, Wang CY, Ward TR, Wilhelmy J, Winzeler EA, Yang Y, Yen G, Youngman E, Yu K, Bussey H, Boeke JD, Snyder M, Philippsen P, Davis RW, Johnston M. 2002. Functional profiling of the Saccharomyces cerevisiae genome. Nature 418:387–391.

32. Roy A, Kucukural A, Zhang Y. 2010. I-TASSER: a unified platform for automated protein structure and function prediction. Nat. Protoc. 5:725–738.

33. **Cingolani G, Petosa C, Weis K, Muller CW.** 1999. Structure of importin-beta bound to the IBB domain of importin-alpha. Nature **399**:221–229.

34. **Imasaki T, Shimizu T, Hashimoto H, Hidaka Y, Kose S, Imamoto N, Yamada M, Sato M.** 2007. Structural basis for substrate recognition and dissociation by human transportin 1. Mol. Cell **28**:57–67.

35. **Cook AG, Conti EI.** 2010. Nuclear export complexes in the frame. Curr. Opin. Struct. Biol. **20**:247–252.

36. **Neville M, Rosbash M.** 1999. The NES-Crm1p export pathway is not a major mRNA export route in Saccharomyces cerevisiae. EMBO J. **18**:3746–3756.

37. **Chook YM, Suel KE.** 2011. Nuclear import by karyopherin-betas: recognition and inhibition. Biochim. Biophys. Acta **1813**:1593–1606.

38. **Görlich D, Dabrowski M, Bischoff FR, Kutay U, Bork P, Hartmann E, Prehn S, Izaurralde E.** 1997. A novel class of RanGTP binding proteins. J. Cell Biol. **138**:65–80.

39. **Lau D, Kunzler M, Braunwarth A, Hellmuth K, Podtelejnikov A, Mann M, Hurt E.** 2000. Purification of protein A-tagged yeast ran reveals association with a novel karyopherin beta family member, Pdr6p. J. Biol. Chem. **275**:467–471.

40. **Pemberton LF, Rosenblum JS, Blobel G.** 1999. Nuclear import of the TATA-binding protein: mediation by the karyopherin Kap114p and a possible mechanism for intranuclear targeting. J. Cell Biol. **145**:1407–1417.

41. **Kakihara Y, Houry WA.** 2012. The R2TP complex: discovery and functions. Biochim. Biophys. Acta **1823**:101–107.

42. **Zhao R, Kakihara Y, Gribun A, Huen J, Yang G, Khanna M, Costanzo M, Brost RL, Boone C, Hughes TR, Yip CM, Houry WA.** 2008. Molecular chaperone Hsp90 stabilizes Pih1/Nop17 to maintain R2TP complex activity that regulates snoRNA accumulation. J. Cell Biol. **180**:563–578.